Effect of Temperature and Transport on the Yield and Composition of Pyrolysis-Derived Bio-oil from Glucose

Khursheed B. Ansari,[1] Jyotsna S. Arora,[1] Jia Wei Chew,[1] Paul J. Dauenhauer,[2] and Samir H. Mushrif [1,3*]

[1] School of Chemical and Biomedical Engineering, Nanyang Technological University, 62 Nanyang Drive, Singapore 637459

[2] Department of Chemical Engineering, University of Minnesota, 425 Washington Ave. SE, Minneapolis, Minnesota 55455, United States

[3] Department of Chemical and Materials Engineering, University of Alberta, 9211-116 St NW, Edmonton, Alberta T6G 1H9, Canada

[*]Corresponding author

Email: mushrif@ualberta.ca (SHM)

Fax: +1 780 492 2881

Tel: +1 780 492 4872

Abstract

Fast pyrolysis of biomass forms bio-oil, char and light non-condensable gases. Bio-oil is the desired product in context of converting biomass to biofuel. The effect of temperature on bio-oil yield and composition is anticipated to be different under reaction-limited and transport-limited operating conditions. Attaining fundamental understanding of the effect of temperature and transport on bio-oil yield and composition is challenging due to limited knowledge of pyrolysis chemistry and inter-relationship between chemistry and transport. In this work, we performed thin-film and powder pyrolysis experiments to investigate the thermal decomposition of glucose (biomass model compound) under both reaction-controlled and transport-limited operating conditions. In thin-film (size $\leq$ 10 μm) experiments, the effect of temperature on pyrolysis product distribution, especially on bio-oil yield and composition, was studied. Additionally, using the thin-film data, mechanistic insights into glucose decomposition were provided and a map of reaction pathways was proposed. Decomposition of glucose in the reaction-controlled regime is initiated by dehydration reactions. With increase in temperature, anhydrosugars, *viz.* levoglucosan and levoglucosenone, apparently converted into furans (hydroxymethylfurfural) and light oxygenates (formic acid/methyl glyoxal), respectively, as ring opening and fragmentation reactions became more facile. Pyrans remained relatively stable. The effect of transport was investigated by performing pyrolysis experiments with different particle sizes. The variation in the yield and composition of bio-oil with respect to temperature and particle size was also analyzed. In the case of glucose powder, levoglucosan yield increased significantly with particle size but decreased marginally with temperature, while hydroxymethylfurfural, furfural, formic acid, and methyl glyoxal yields monotonically increased with increase in temperature and particle size. Thin-film of glucose gave lower yield of bio-oil and higher yield of char than that of glucose powder.

Keywords: Glucose, pyrolysis, Thin-film, Powder, Bio-oil, Reaction-controlled, Transport-limited

1. Introduction

Fast pyrolysis process rapidly heats biomass to elevated temperatures (400 – 1000 ºC) in the absence of oxygen to produce volatile organic products and char. The volatile products (except non-condensable gases) are later condensed to form bio–oil.[1] Compared to gasification and biochemical conversions, pyrolysis is suggested to be more economical due to its low operating and capital cost.[2] Pyrolysis of biomass also offers the unique advantage of distributed processing of biomass. The product bio-oil can be later upgraded for use as a fuel in heating and transportation sectors.[3-6] Moreover, pyrolysis generates lower anthropogenic carbon dioxide emissions, contributes less to SO*x* (sulfur oxides) emissions, generates light gases for energy applications and biochar for soil amendment, and offers reduction in the emission of dioxins and in the generation of ash.[3, 7]

Despite being a promising platform to produce renewable biofuel and/or chemicals, the commercialization of biomass pyrolysis technique is hindered by challenges in systematically optimizing the operating conditions (i.e. temperature and feedstock particle size) and the reactor design for different biomass feedstocks. It is reported that lower temperature (~ 300 ºC) yields more char,[8, 9] while the temperature between 500 ºC – 550 ºC produces a higher yield of bio-oil.[8-14] At temperatures above 600 ºC, bio-oil yield decreases with increase in non-condensable gases *via* secondary decomposition reactions. The optimum temperature for maximum bio-oil yield changes with feedstock, in the range of 400 ºC and 600 ºC.[8, 11-14] However, the operating temperature not only changes bio-oil yield but also changes its composition.

Pyrolysis derived bio-oil consists of hundreds of compounds and the composition varies with operating conditions (i.e. operating temperature and feed particle size) and the reactor design. The chemical composition of bio-oil determines its stability, quality, suitability for downstream processing (or upgrading) and environmental impact (after the burning of bio-oil). The composition of bio-oil is also be important as characterized by the following descriptors:

(i) *Oxygen content*: Bio-oil comprises of oxygenated compounds and exhibit high oxygen content (30 – 50 wt % of bio-oil).[10, 15-17] The oxygen content makes it unstable, reactive and corrosive in nature, with low heating value. Higher oxygen content in bio-oil also means more hydrogen for its upgrading. Hence, for utilizing pyrolysis bio-oil as a fuel, it is desirable to minimize oxygen containing compounds like anhydrosugars, pyrans, low molecular weight oxygenates (acids/alcohols/aldehydes/ketones) and oxygenated furans.

(ii) *Environmental point of view:* Bio-oil may contain small amounts of hazardous compounds like dioxins. Dioxins can cause serious health issues like cancer and reduced immunity.[18]

(iii) *Chemical point of view:* Despite hundreds of compounds present in bio-oil, few exists in higher concentrations. Levoglucosan (anhydrosugar), furfural and hydroxymethylfurfural (furanic compounds), methyl glyoxal and hydroxyacetone (light oxygenates) are examples of predominant compounds present in the bio-oil derived from pyrolysis of cellulosic biomass.[19-21] Depending on the biomass initial composition and pyrolysis conditions, the selectivity of these compounds can be tuned.

Obtaining the desired yield and composition of bio-oil (with different feedstocks) is challenging and requires systematic understanding of the effect of pyrolysis operating conditions such as temperature and feedstock particle size. Deconvoluting the effect of temperature and transport (which arises due to different particle sizes of biomass feed) on the

yield and composition of bio-oil is difficult, because the operating temperature not only affects pyrolysis chemistry but also transport limitations such as diffusion and heat transfer.

Pyrolysis particle models capturing transport frequently fail to describe intrinsic reaction chemistry.[22-28] Multiple pathways of biomass decomposition have been proposed by taking glucose, cellulose, cellobiose, methyl-cellobiose, cellotriose, glycerol, and α-cyclodextrin as model compounds[19, 20, 29-40] but most of the pathways/mechanisms require experimental validation. Moreover, if a kinetic/microkinetic model is developed based on proposed reaction mechanisms, it is unlikely to reproduce the experimental pyrolysis product distribution (which is obtained under pyrolysis conditions free of transport limitations).

Additionally, unlike cellulose and α-cyclodextrin, it is extremely challenging to measure glucose decomposition kinetics using the state of the art method like Pulse-Heated Analysis of Solid Reactions (PHSAR) reactor due to very fast decomposition of glucose.[29, 30] Hence, there is no direct way of measuring reaction mechanisms and kinetics for glucose. However, glucose pyrolysis, if performed under reaction-controlled regime (or thin-film scale), can provide the information about its decomposition mechanisms as a function of operating temperature, while, transport-limited (or powder) pyrolysis of glucose can reveal the effect of transport on the yields of individual pyrolysis products at different temperatures.

Due to the need of a systematic study of the effects of temperature on the yield and composition of bio-oil, with and without transport limitations, we examine here thin-film (transport-limitation free and reaction-controlled regime) and powder (transport-limited) pyrolysis using glucose as a model compound. Glucose decomposition chemistry is characterized and a detailed reaction map is proposed based on the data from thin-film pyrolysis of glucose. By varying the size of glucose particles (ranging from 10 μm to 523 μm), experiments are performed to evaluate the effect of transport, coupled with the operating temperature on the pyrolysis product distribution. The effect of pyrolysis operating conditions

(i.e. operating temperature and glucose particle size) on the yield and composition of bio-oil is analyzed.

2. Experimental Description

2.1. Material and sample preparation

Glucose in powder form (Part number: G8270) was acquired from Sigma Aldrich, Singapore. A thin-film of glucose was prepared by dissolving 1.0 % (weight basis) of glucose in deionized water. Then, 25 μL of 1.0 wt % clear glucose solution was transferred into a cylindrical pyrolysis crucible of size 4 mm × 8 mm (diameter × height). The water was then removed *via* room temperature evacuation, leaving behind a micro-meter sized film of glucose on the inner wall of the crucible.[19] The thickness of the glucose film was measured using digital microscope (Leica DVM6) and Scanning Electron Microscope (SEM), respectively, as shown in Figures 1 [A] and 1 [B]. The image analysis showed glucose film thickness of 8 – 10 μm, which falls inside the reaction-controlled regime of pyrolysis.[20]

To prepare powder samples, 0.25 mg of glucose was weighed using a micro-balance (OHAUS AX224 series) and then deposited directly into the pyrolysis crucible. The particle size distribution of glucose powder was measured by Partica LA-960 series (Horiba Scientific equipment). As compared to the thin-film (size ≤ 10 μm) samples, the glucose particles in the powder form ranged between 10 – 523 μm (*cf* Figures 2 [A] and 2 [B]). Two distinct particle size distributions *viz.* 83 – 523 μm (*cf* Figures 2 [A]) and 10 – 262 μm (*cf* Figures 2 [B]) were measured for glucose powders, which fall outside the reaction-controlled pyrolysis regime.[20]

2.2. Pyrolysis experiments and product identification

Glucose thin-film and powder samples were pyrolyzed using a micropyrolyzer (PY-3030S single shot pyrolyzer, Frontier Laboratories Ltd., Japan). The heating rate of glucose thin-film samples (size ≤ 10 microns) in micropyrolyzer is estimated to be about 1,000,000 ^{o}C/min,[20] which is 3 – 5 orders of magnitude faster than traditional heating rates in pyrolysis

techniques. For glucose powders (size = 10 – 523 micron), the estimated heating rate is about 10800 ºC/min,[41] which requires about 1 – 2 seconds to attain the desired pyrolysis temperature (i.e. 500 ºC). Pyrolysis volatile products were identified and quantified using Agilent Gas Chromatograph (7890B) coupled with Mass Spectrometer (5977B MSD), as shown in Figure S1 in the supporting information. The summary of identified pyrolysis products in glucose thin-film/powder pyrolysis experiments is provided in Table T1 of the supporting information. Volatile products (comprising of condensable bio-oil and non-condensable gases) were swept from the hot reactor zone to the gas chromatograph, immediately after their generation, using a continuous flow of helium gas. Later, they were isolated using multidimensional chromatography technique, while post-reaction, the solid residue of pyrolysis (char) was quantified *via* combustion by injecting the oxygen pulse into the micropyrolyzer.[19, 20] The equivalent amount of combustion gas (mostly identified as carbon dioxide) was accounted for char quantification. The volatile products of glucose pyrolysis were identified using both, mass spectrometry and by comparing retention times (RT) of these compounds to that of pure standards. The RT analysis of six compounds (*viz.* dianhydroglucopyranose (DAGP); 1,6-anhydroglucofuranose (AGF); 1,5-anhydro-4-deoxy-D-glycerohex-1-en-3-ulose (ADGH); 2,3-dihydro-3,5-dihydroxy-6-methyl-4HPyran-4-one (DHMDHP); 1,2-cyclopentanedione (CPD); 2-hydroxy-3-methyl-2-cyclopenten-1-one (CPMH)) could not be performed as they were locally unavailable and were identified using mass spectrometry only. The calibration for these six compounds was done using structurally similar compounds (in terms of C/O ratio, functional groups, cyclic/noncyclic) with the same number of carbons.[19, 20] Both thin-film and powder pyrolysis experiments were conducted in triplicate and the average values (product yields, % C basis) are shown in section 3 with experimental error. The standard deviation in individual product yields ranged between 2 – 3 %. The overall carbon balance for thin-film and

powder pyrolysis of glucose, including non-condensable gases, condensable volatiles and char, was 77% and 83%, respectively.

3. Results and Discussion

In section 3.1, overall product yields (*viz.* percentages of non-condensable gases, bio-oil and char) and the yields of individual bio-oil compounds (*viz.* anhydrosugars, pyrans, furans and light oxygenates) from glucose thin-film (reaction-controlled) and powder (transport-limited) pyrolysis experiments are compared. The effect of temperature (in the reaction-controlled regime) on the yields of individual bio-oil compounds and on non-condensable gases and char are discussed in sections 3.2 and 3.3, respectively. Based on the product distribution of glucose thin-film pyrolysis at different temperatures, insights into glucose decomposition mechanisms are provided and a detailed reaction map is presented in section 3.4. Section 3.5 discusses glucose powder pyrolysis data (under different particle sizes) with the effect of transport-limitations and temperature on bio-oil composition. The change in non-condensable gases and char yields with respect to temperature and particle size is described in section 3.6. A comparison of glucose thin-film/powder pyrolysis results obtained in the current work with the cellulose pyrolysis performed under similar operating conditions, is provided in section 3.7. Lastly, optimum pyrolysis operating conditions (i.e. temperature and particle size) for glucose-derived products, especially for bio-oil compounds, are discussed in section 3.8.

3.1. Comparison of overall product distribution and bio-oil components in thin-film and powder pyrolysis

Fast pyrolysis of glucose in the reaction-controlled regime (thin-film) at 300 ºC – 500 ºC yielded non-condensable gases (0.15 – 3.7 %), condensable volatile compounds (bio-oil, 21 – 50 %), and char (25 – 56 %), as products (*cf* Table 1 [A]). The non-condensable gases were comprised of carbon dioxide (CO_2 ~ 2 %) and carbon monoxide (CO ~ 1.6 %) at low yield, but it increased with increase in the pyrolysis temperature.[19] The condensable volatile

compounds collectively form bio-oil and are broadly categorized into anhydrosugars, pyrans, furans and light oxygenates. The yield of bio-oil derived from glucose thin-film pyrolysis increased by almost 30 % while the yield of char decreased (~ 31 %) with increasing pyrolysis temperature (300 ºC to 500 ºC), as shown in Table 1 [A].[19, 20] Within the pyrolysis bio-oil, anhydrosugars decreased by 32 % over 300 ºC – 500 ºC and a similar increase (~ 31 %) was observed in light oxygenate yields, while furans and pyrans yields changed marginally at higher operating temperature (~ 500 ºC) of pyrolysis (*cf* Table 1 [B]). The powder form of glucose (particle sizes = 10 – 262 µm and 83 – 523 µm, transport-limited) produced similar yields of non-condensable gases (0.33 – 6 %), but higher yields of condensable volatile compounds (16 – 26 %) and a lower yield of char (12 – 35 %), as compared to glucose thin-film (*cf* Table 1 [A]). Non-condensable gases (CO_2:~ 0.3 – 3.2 % and CO:~ 0.1 – 3.07 %) still remained low in quantity but showed increasing trend over the pyrolysis temperatures. The yield of total condensable volatiles (constituting bio-oil) increased (~ 17 – 20 %) with an increase in the pyrolysis temperatures from 300 ºC to 500 ºC, while char yield decreased (~ 18 – 20 %) over a similar range of temperatures (*cf* Table 1 [A]). Similar to glucose thin-film pyrolysis, the yield of anhydrosugars in the bio-oil of glucose powders reduced significantly (~ 25 %) with increasing pyrolysis temperatures, which can be ascribed to its subsequent decomposition reaction to produce furans and light oxygenates (Table 1 [B]).[31] This is also evident from the increase in light oxygenate yields (~ 26 %) for powder samples of glucose over 300 to 500 ºC, as shown in Table 1 [B]. Further, pyrans derived from glucose powders did not change significantly over the entire operating temperatures but furans exhibited a slight decrease in their yields at higher temperature (~ 500 ºC).

It was observed that the yield of bio-oil obtained from glucose thin-films was significantly lower than that obtained from glucose powders at all temperatures (*cf* Table 1 [A]). The bio-oil yields, on a carbon basis, competes with non-condensable gases and char production and

for higher yields of either pyrolysis gases or char, the bio-oil yield is compromised.[19] Additionally, the uniform and/or isothermal temperature within glucose thin-films apparently leads to the repolymerization of primary pyrolysis products or intermediates and hence contributes to higher char formation.[19, 42] The discussion on higher char formation in glucose thin-film pyrolysis is provided later in this paper (section 3.6). Further, anhydrosugars obtained from the pyrolysis of glucose powders remained slightly higher than those obtained from glucose thin-film (Table 1 [B]). Anhydrosugars tend to convert into lighter compounds at higher pyrolysis temperature (~ 500 ºC) and the uniform (high) temperatures within glucose thin-films assist its further decomposition. On the other hand, thermal gradient in glucose powders may not facilitate the decomposition of anhydrosugars. This was also evident from the higher yields of light oxygenates at 500 ºC in glucose thin-film pyrolysis.

3.2. Glucose thin-film pyrolysis: Effect of pyrolysis temperature on bio-oil composition

Anhydrosugars in bio-oil derived from glucose thin-film pyrolysis consisted of levoglucosan (LGA), 1, 6-anhydroglucofuranose (AGF), dianhydroglucopyranose (DAGP) and levoglucosenone (LGO), as shown in Figure 3 [A]. The yields of LGA and LGO decreased by 2 – 3 %, while that of AGF and DAGP showed marginal increase (1 – 2 %) with increase in the pyrolysis temperature from 300 °C to 500 °C. The furanic compounds of bio-oil consisted of 5-hydroxymethylfurfural (HMF), furfural, 2-furanmethanol, 2-methylfuran, furanone, 2(5H), furan, 5-methylfurfural and 2, 5-dimethylfuran, as shown in Figures 3 [B] and 3 [C]. Major furans like HMF and furfural increased with an increase in the temperature, while amongst minor furanic compounds (having % C yield ≤ 1) 2-methylfuran, 2-furanmethanol, 2, 5-dimethylfuran, and furan showed an increase in their yields; furanone, 2(5H) and 5-methylfurfural indicated decreased yields at higher temperature (500 ºC) (*cf* Figures 3 [B] and 3 [C]). The light oxygenates of bio-oil consisted of formic acid (FA), methyl glyoxal (MG), hydroxyacetone (HAA), 1, 2-cyclopentanedione (CPD), glyoxal (GL), acetic acid (AA), 2-

hydroxy-3-methyl-2-cyclopenten-1-one (CPHM) and 2, 3-butanedione (BD) (*cf* Figures 3 [D] and 3 [E]). FA, MG, CPD and HAA collectively formed major light oxygenates (~ 7 – 18 %), while AA, BD, GL and CPHM remained lower in quantity (~ 2 – 2.5 %) and was designated as minor light oxygenates. FA, MG and HAA tended to increase with increasing pyrolysis temperatures, while CPD decreased (~ 2.95 %) beyond 400 ºC and a similar increase in the collective yields of BD and AA (~ 2 %) was observed. Amongst minor light oxygenates, AA, BD and GL continued to increase with an increase in the pyrolysis temperatures, while CPHM yield decreased (~ 1.2 %) after 300 ºC. The pyrans present in bio-oil comprised of 1, 5-anhydro-4-deoxy-D-glycerohex-1-en-3-ulose (ADGH) and 2, 3-dihydro-3, 5-dihydroxy-6-methyl-4HPyran-4-one (DHMDHP). Both ADGH and DHMDHP increased marginally (0.38 – 0.46 %) over the entire range of pyrolysis temperatures (*cf* Figure 3 [F]).

3.2.1. Effect of temperature on the yield of anhydrosugars

LGA, a dehydration product of glucose, is formed by the loss of C_1/OH and H from the C_6/OH group.[42] Our experimental results showed that the yield of LGA remains higher at low pyrolysis temperature (~ 300 ºC). The conversion of glucose-based carbohydrates into LGA requires an activation barrier in the range of 48 – 59 *kcal/mol*[34, 36, 42] which is attainable at around 300 ºC under conditions free of transport limitations; hence, LGA was observed in higher amount. However, when pyrolysis temperature increased to 400 ºC, LGA yield decreased and another product, HMF, increased. The decrease in LGA yield (~ 1.88 %) between 300 ºC – 400 ºC was compensated by the increase in the HMF yield (~ 1.9 %) (Figure S2 of the supporting information), showing that LGA (or anhydrosugar) is apparently an intermediate for HMF formation. The glucose-derived dehydrated species (or intermediates) can convert into either LGA or HMF as final products, but the barrier for HMF formation (45 – 73 *kcal/mol*)[43, 44] was slightly higher than that of LGA formation (48 – 59 *kcal/mol*).[34, 36, 42]

Hence at low temperatures, LGA yield is higher; but at 400°C and higher temperatures, LGA further decomposed to form HMF.

LGO, another dehydration product of glucose, can also form *via* the LGA intermediate path or directly from glucose.[34, 42] Our experimental results suggest that LGO forms directly from glucose instead of following the LGA intermediate path. The increase in experimental yield of LGO never compensated with simultaneous decrease of LGA yield over the entire range of operating temperature (Figure S2 of supporting information). Furthermore, the reported barrier for conversion of LGA to LGO (~ 69 *kcal/mol*)[34] is significantly higher than glucose direct decomposition into LGO (42 – 50 *kcal/mol*, barrier),[42] which makes LGO formation *via* the LGA intermediate path kinetically more difficult within the operating temperature of pyrolysis. However, a decrease in LGO yield around 500 ºC indicated its further decomposition, contributing to methyl glyoxal (MG) and formic acid (FA) formation, because the decrease in LGO yield (~ 3.26 %) was compensated by the collective increase in MG and FA yields (~ 3.7 %) (Figure S2 of supporting information). Further, the barriers for FA and MG formation (37 – 57 *kcal/mol*)[42, 45] *via* multiple reactions of anhydrosugars are attainable at around 500 ºC temperature.

Next, the yields of DAGP and AGF increased marginally over the pyrolysis temperature range. The formation of DAGP and AGF from glucose has a barrier of 32 – 50 *kcal/mol*[42] which can be easily achieved in between 300 ºC to 500 ºC operating temperatures and under isothermal pyrolysis conditions. However, unlike LGA and LGO, both AGF and DAGP did not undergo secondary reactions over entire pyrolysis temperature (*cf* Figure 3 [F]).

3.2.2. Effect of temperature on the yield of furans

HMF can be generated from glucose *via* multistep reactions involving glucose isomerization (33 – 37 *kcal/mol*) and dehydration (38 – 56 *kcal/mol*).[35, 42, 46-51] Amongst the various possible pathways reported for HMF, the fructose intermediate path is proposed to be

more favourable than the direct conversion of glucose,[43, 47, 52] or *via* anhydrosugars (LGA) intermediate path.[42, 44] Our experimental results showed that until 400 ºC, HMF was formed *via* the anhydrosugars intermediate path. At higher temperature, the HMF yield increased continuously and did not match with the change in yield of LGA, indicating HMF formation occurred predominantly from the direct decomposition of glucose, instead of following the anhydrosugar path (Figure S3 of supporting information). Glucose-based carbohydrates can decompose directly into HMF by overcoming a barrier of 56 *kcal/mol*[42]; The formation of HMF directly from glucose is more facile at higher temperatures (~ 500 ºC) of pyrolysis. Once HMF is formed, it can convert into furfural *via* deformylation reaction (62 *kcal/mol*, barrier),[42] which was evident from the low yield (~ 0.5 %) of HMF and high yield of furfural (~ 4.2 %) at 300 ºC. However, as pyrolysis temperature increased, furfural continued to increase but a corresponding decrease in HMF yield was not observed suggesting that, furfural too could form *via* direct decomposition of glucose with a 47 – 57 *kcal/mol* [42] barrier, which is attainable between 400 ºC to 500 ºC. HMF and furfural also contribute to the formation of minor furanic compounds *viz.* 2-furanmethanol, furan, furanone, 2(5H), 2, 5-dimethylfuran, 2-methylfuran, and 5-methylfurfural (yield < 1%).[42] However, any insights on the competing pathways resulting in any of these minor oxygenated and/or deoxygenated furanic compounds could not be drawn because of their lower yields.[31, 43, 47, 52]

3.2.3. Effect of temperature on the yield of light oxygenates

The predominant light oxygenates like FA and MG can be derived from glucose by overcoming the rate limiting barriers of 52 *kcal/mol* and 57 *kcal/mol*, respectively.[42] Beyond 400 ºC, these barriers (52 – 57 kcal*/mol*) can be readily overcome, consistent with observed higher yields of FA and MG (~ 500 ºC). The comparison between experimental yields of light oxygenates and anhydrosugars suggested that the light oxygenates could be mainly obtained from anhydrosugars (*via* secondary decomposition reaction)[42], and we also observed the

secondary decomposition of LGO to FA and MG at around 500 ºC (Figure S4 of supporting information). Additionally, Broadbelt et al., also proposed that anhydrosugars could convert into light oxygenates by overcoming a barrier of ~ 62 *kcal/mol*[42], which is attainable at 500 ºC. Unlike FA and MG, the light oxygenates CPHM and CPD exhibited different trends and remained higher in yield at 300 ºC and 400 ºC, respectively. But beyond 400 ºC, they further decomposed into AA, HAA, BD and GL, by overcoming a barrier of 60 – 62 *kcal/mol*[42] (Figure S4 of supporting information). AA, HAA, BD and GL yields continued to increase at higher pyrolysis temperatures.

3.2.4. Effect of temperature on the yield of pyrans

Yield of ADGH and DHMDHP (collectively designated as pyrans), increased marginally (0.38 – 0.46 %) over the pyrolysis temperature range (*cf* Figure 3 [F]). ADGH and DHMDHP are formed through series of dehydration steps of glucose with 68 – 69 *kcal/mol*[53] and 89 *kcal/mol* barriers, respectively. Unlike anhydrosugars (*viz*. LGA and LGO), ADGH and DHMDHP remain stable and do not undergo secondary reactions to form lighter oxygenates, even with an increase in the pyrolysis temperature (*cf* Figure 3 [F]).

3.3. Glucose thin-film pyrolysis: Effect of pyrolysis temperature on non-condensable gases and char

Non-condensable gases consisting of CO_2 and CO remained low in yield but exhibited increasing trend in yield over 300 ºC – 500 ºC (*cf* Figure 3 [F]). The suggested barriers (40 – 62 *kcal/mol*)[42] for both CO_2 and CO formation from glucose *via* different competing pathways can be easily achieved at higher temperatures (~ 500 ºC), thus increasing the yield of non-condensable gases. The yield of char decreased with an increase in pyrolysis temperature (*cf* Figure 3 [F]), which can be correlated with the yield of bio-oil. The yield of char, on a carbon basis, also competes with other pyrolysis products (i.e. bio-oil and non-condensable gases

yields).[19] Since the yield of bio-oil is increased with an increase in temperature, it also resulted in the reduction in char yield.

3.4. Reaction map of glucose thin-film pyrolysis products

A reaction map for glucose thin-film pyrolysis (reaction-controlled regime) derived products, over 300 ºC – 500 °C is proposed and is shown in Figure 4. At lower temperature (~ 300 ºC), glucose majorly converted into anhydrosugars (LGA, LGO, AGF and DAGP), pyrans (ADGH and DHMDHP), furan (furfural *via* HMF intermediate path) and solid residue (char). This indicated that the primary decomposition of glucose around 300 ºC was initiated *via* dehydration while, the solid residue (or char), at 300 ºC still contained some unconverted mass of glucose. In between 300 ºC to 400 ºC, LGA or anhydrosugars of glucose pyrolysis converted into furanic compounds (*viz.* HMF), indicating that a glucose dehydration intermediate also exhibited ring-opening/closing reactions at around 400 ºC to form furanic compounds. Within the similar range of operating temperature (300 ºC to 400 ºC), AGF, DAGP and LGO (anhydrosugars) and ADGH and DHMDHP (pyrans) continued to form from glucose *via* multiple dehydration/tautomerization reactions,[42] but their yields changed marginally (0.1 – 0.6 %) showing that the aforementioned anhydrosugars and pyrans formation from glucose was still favorable at 400 ºC.

Beyond 400 °C, anhydrosugars (*viz.* LGO and LGA) apparently broke down into light oxygenates (FA and MG), while, the major furans (*viz.* HMF and furfural) continued to form *via* direct decomposition of glucose.[42] This showed that glucose pyrolysis reactions responsible for furanic compounds and ring opening/fragmentation compound formation were favourable at higher operating temperature (~ 500 ºC). Further, the major furans (*viz.* HMF and furfural) to some extent also converted into minor furans (< 1% C basis) between 300 ºC to 500 ºC. Amongst light oxygenates, CPD and CPHM (cyclic oxygenates) decrease beyond 400 ºC and converted into linear oxygenates like HAA, AA, BD and glyoxal formation which also

provided an evidence for the ring fragmentation reactions at higher temperatures. The non-condensable gases (CO and CO_2) were generated from glucose (predominantly *via* decarbonylation reactions)[42] in between 300 ºC to 500 ºC, while char could also form within the similar range of pyrolysis temperature, as shown in Figure 4.[42] Glucose thin-film derived dehydrated products (as intermediates) also likely contributed to char formation *via* repolymerization reactions, as shown with red lines in Figure 4. The discussion on char formation is provided in section 3.6.

3.5. Pyrolysis of glucose powder: Effect of transport on bio-oil composition

3.5.1. Effect of transport on the yields of anhydrosugars and pyrans

The powder form of glucose with different particle size distributions (10 – 262 µm and 83 – 523 µm) produced different yields of LGA, AGF, DAGP and LGO between 300 ºC to 500 ºC, as shown in Figure 5 [A, B, C and D]. LGA yield deceased marginally (1 – 2 %) with temperature but increased significantly (~ 9 % for increment in particle size from 10 – 262 µm size to 83 – 523 µm and ~ 16 % for 8 – 10 µm (as thin-film) to 83 – 523 µm), with increasing size of glucose particles (*cf* Figure 6 [A]). Unlike LGA, the yield of AGF increased marginally (~ 2 %) with an increase in particle size until 400 ºC; but beyond that temperature, AGF obtained from glucose powders (10 – 262 µm and 83 – 523 µm) apparently remained similar to that of the glucose thin-film experiments (*cf* Figure 5 [B]). DAGP yield increased marginally (0.45 – 0.96 %), while, the yield of LGO decreased, with an increase in temperature and particle size of glucose (including thin-film and powder scale), as shown in Figure 5 [C and D], respectively. DHMDHP yield showed a decreasing trend with increasing particle size, while ADGH yield showed the reverse trend, over 300 °C to 400 °C, as shown in Figure 5 [E] and 5 [F]. At higher temperature of pyrolysis (~ 500 °C), ADGH and DHMDHP yields became similar for both glucose powders and thin-film samples.

Glucose powders possessed an internal temperature gradient (due to differences in external/internal heat transfer time-scale), which became more pronounced with particle sizes.[19, 23, 24, 54] The thermal gradient resulted in a lag-phase for attaining the desired reaction temperature (~ 500 °C) within these particles, which varied between 100 to 1000 milliseconds (size of particles ≈ 780 μm) and almost one order of magnitude higher than the thin-film (≤ 10 μm) samples (where it is <100 millisecond).[19] The differences in heat transfer time-scales (or thermal gradient within the particle), as a function of the characteristic size of glucose particles created transport-limitations which affected the pyrolysis reaction rates and hence the final product yields. The increments in LGA yield with increasing particle size could be attributed to its stability under transport-limited operating conditions (*cf* Figure 5 [A]). AGF and DAGP yields suggested that the AGF formation from glucose behaved differently over 300 °C to 500°C under transport-limited conditions, while yields of DAGP showed linear relationship (or increased) with temperature and glucose particle sizes (*cf* Figures 5 [B] and 5 [C]). Moreover, the decreasing yield of LGO with temperature and particle size indicated its further decomposition into lighter compounds in both the reaction-controlled and transport-limited pyrolysis conditions. The DHMDHP formation apparently decreased under the transport-limited condition (or increasing size of glucose particle) but did not change significantly with temperature; while, the yield of ADGH increased with increasing particle size, (*cf* Figure 5 [E] and 5 [F]). At 500 °C, ADGH and DHMDHP formation from glucose became similar for both the reaction-controlled (thin-film) and transport-limited (powder) operating conditions. In brief, the glucose ring opening/closing and dehydration reactions which govern the formation of anhydrosugars and pyrans, behaved differently for each of the dehydrated products under transport-limited pyrolysis conditions.

3.5.2. Effect of transport on the yield of furanic compounds

The yields of major furanic compounds (*viz.* HMF and furfural) increased until 400 ºC with an increase in the glucose particle size, as shown in Figures 6 [A] and [B]. HMF increased by 4 – 7 % with an increase in the size of glucose powder from 10 – 262 µm to 83 – 523 µm. HMF also increased by 8 – 9 % for the maximum size of glucose powders (83 – 523 µm) than glucose thin-film (8 – 10 µm). Unlike HMF, the furfural yield increased by 2 – 5 % with an increase in glucose particle sizes until 400 ºC. However, at 500 ºC, HMF and furfural yields from glucose powders decreased (~ 5 %), indicating their further decomposition into minor furanic compounds. The minor furans (yield < 1 %) like 5-methylfurfural, 2-methylfuran and furan showed increased yields, whereas 2, 5-dimethylfuran, furanone, 2(5H) and 2-furanmethanol showed lower yields with an increase in the size of glucose powder, as shown in Figure 6 [C to H].

Furanic compounds are reportedly formed from glucose-based carbohydrates either *via* fructose intermediate or anhydrosugars pathway.[16, 31, 32, 36-41] Our experimental results showed that up to 400 ºC, HMF and furfural yields increased significantly with increasing size of glucose particles; but beyond that temperature (or around 500 ºC), it decreased and became similar to the yields obtained from glucose thin-film pyrolysis. This indicated that at higher temperatures, both HMF and furfural apparently decomposed into other furanic compounds. Amongst minor furanic compounds, the formation of 5-methylfurfural, 2-methylfuran and furan formations apparently increased, while, 2, 5-dimethylfuran, 2-furanmethanol and furanone, 2(5H) formation decreased under transport-limited pyrolysis of glucose over 400 ºC – 500 °C.

3.5.3. Effect of transport on the yield of light oxygenates

The yields of major light oxygenates like FA and MG increased slightly (1 – 3 %) with an increase in the size of glucose powder (from 10 – 262 µm to 83 – 523 µm) at 400 ºC – 500 °C, as shown in Figures 7 [A] and 7 [B]. Minor light oxygenates (HAA, AA and BD), except

glyoxal, showed the reverse trend in their yields as compared to the major ones (*cf* Figures 7 [C to F]). The yield of glyoxal increased with an increase in glucose particle size, albeit only at higher pyrolysis temperatures (~ 500 °C) (*cf* Figure 7 [C]). The yields of CPD and CPHM decreased marginally (~1 %) with an increase in glucose particle size, over the entire range of pyrolysis temperatures (*cf* Figures 7 [G] and 7 [H]). FA and MG yields increased linearly with increasing pyrolysis temperatures and glucose particle size, indicating both FA and MG formation from glucose were slightly enhanced under transport-limited pyrolysis, over 400 °C to 500 °C. This was further supported with the apparent decrease in the yields of minor light oxygenates (HAA, AA and BD, except glyoxal) with increasing size of glucose particle between 400 °C to 500 °C.

3.6. Effect of transport on the yields of non-condensable gases and char

The yield of non-condensable gases (CO and CO_2) obtained from the pyrolysis of glucose powders increased marginally (1 – 2 %), at 400 °C to 500 °C (*cf* Figures 8 [A] and 8 [B]). The char yield showed a decreasing trend over the pyrolysis temperature, for both glucose powder and thin-film samples, but char yield remained higher in glucose thin-films as compared to that of glucose powders (*cf* Figure 8 [C]). By comparing char yield with variation in bio-oil compounds, we found that the decrease in char yield for glucose powder samples compared to glucose thin-film was in good agreement with the cumulative increase in the yield of anhydrosugars (LGA, AGF and DAGP) and pyrans (ADGH) (Table T2 of the supporting information), suggesting that anhydrosugars/pyrans from glucose thin-film pyrolysis apparently undergo repolymerization to contribute to char formation. The repolymerization of anhydrosugars/pyrans species was likely promoted by uniform temperature within the glucose thin-film.

3.7. Glucose thin-film and powder pyrolysis: Comparison with cellulose pyrolysis

Biomass pyrolysis reports investigating the effect of temperature on bio-oil yield and composition, with and without transport limitations, used cellulose/carbohydrate-based material as feedstocks due to their abundance in biomass.[19, 20, 55] It is useful to compare the decomposition of glucose (described in the present work) with pyrolysis temperatures and particle sizes with that of cellulose decomposition under similar reaction conditions. Despite being a monomer of cellulose, the choice of glucose as a model compound for cellulose is still debated in the literature and its thermal decomposition chemistry, with and without transport, needs to be compared with that of cellulose. Our experimental results suggested that glucose pyrolysis produced lower yield of bio-oil than cellulose pyrolysis conducted under similar operating conditions. Further, the primary decomposition of glucose was initiated by dehydration reactions, producing anhydrosugars/pyrans in higher amounts. The pyrolysis of cellulose also produced LGA (*via* dehydration reaction) in major quantity, but the yield of LGA obtained from glucose in the current work was significantly lower than the yield of LGA from cellulose pyrolysis.[19, 31]

Additionally, HMF derived from thin-film pyrolysis of glucose increased with an increase in the pyrolysis temperature, which was in contrast with the HMF trend obtained during cellulose thin-film pyrolysis at similar operating temperatures (300 ºC to 500 ºC).[19] Furthermore, the powder samples of glucose (under transport-limited conditions) showed a similar trend in HMF yield as that of cellulose powders. The formation of HMF from glucose could proceed *via* two competing pathways (the LGA intermediate path and direct decomposition of glucose), that are strongly dependent on the pyrolysis temperature, as discussed in section 3.2. In cellulose, it was reported that pyranose ring opening was accompanied by glycosidic bond cleavage to form 5-membered intermediates which eventually converted to furanic compounds.[20] Unlike HMF, furfural yields remained slightly higher (~ 2.5 %) in glucose thin-film and powder pyrolysis experiments than that of cellulose pyrolysis.[19]

Light oxygenates are formed in higher amounts at 500 ºC from pyrolysis of both thin-film and powder samples of glucose and cellulose,[19] indicating that the secondary decomposition reactions of glucose/cellulose compounds, occur at higher pyrolysis temperatures. However, glucose pyrolysis produced FA and MG as major light oxygenates, while, cellulose converted into FA, MG, HAA and formaldehyde as predominant light oxygenates, under similar operating conditions. Moreover, the comparison between char yields, obtained from both glucose and cellulose pyrolysis (in thin-film and powder samples), suggested that the yield of glucose-derived char remained higher than cellulosic char (12 – 36 %) for all temperatures (300 ºC – 500 ºC).[19] The char yield can be further correlated with the yields of anhydrosugars (i.e. LGA) for both the feedstocks, where LGA remained higher for cellulose pyrolysis than that of glucose.

In brief, the pyrolysis of glucose under reaction-controlled (thin-film) and transport-limited (powders) conditions produced similar products to that of cellulose pyrolysis[19], but the yields of individual products (i.e. LGA and HMF/furfural) within bio-oil were significantly different.

3.8. Glucose thin-film and powder pyrolysis: Optimum operating regimes

The product distributions obtained from glucose thin-film and powder pyrolysis experiments are interpolated with a thin-plate spline method, to evaluate the optimum operating regimes for glucose-derived products, especially bio-oil. The interpolated yields of non-condensable gases, char, bio-oil and bio-oil compounds (*viz.* furans, HMF, furfural, anhydrosugars, and LGA) are shown in figure 9. The non-condensable gases are maximized at higher pyrolysis temperature (~ 500 ºC) and with larger glucose particles (~ 460 – 500 µm), as shown in Figure 9 [A]. Similar to non-condensable gases, the yield of bio-oil remains high at 500 ºC and under transport-limited conditions (glucose powders ~ 500 µm), and it is the lowest at 300 ºC in thin-film (*cf* Figure 9 [B]). The yield of char showed the reverse trend to that of

bio-oil/non-condensable gases and was the lowest at 500 ºC and around 500 µm particle size (*cf* Figure 9 [C]).

In the context of bio-oil quality and/or composition, the furans in bio-oil were maximized at around 500 ºC and with the particle size ~ 300 µm (*cf* Figure 9 [D]). HMF, a predominant furanic product, was also maximized at around 500 ºC and with 200 – 400 µm particle size, indicating its generation competes with other furans in glucose-derived bio-oil (*cf* Figure 9 [E]). Furfural yield remained high at around 400 ºC and with 200 – 300 µm particle size (*cf* Figure 9 [F]). Anhydrosugars and the predominant compound (*viz.* LGA),[19, 31] can be maximized at around 500 ºC and with 460 – 500 µm particle size (*cf* Figures 9 [G and H]). In summary, we showed that by tuning particle size and temperature, the yield and composition of bio-oil could be altered. Such optimization of pyrolysis operating conditions (i.e. temperature and particle size) would aid in improving the yield and the composition of bio-oil obtained from pyrolysis processes.

4. Conclusions

In this work, we investigated the pyrolysis of glucose under reaction-controlled (thin-film pyrolysis) and transport-limited (powder pyrolysis) operating conditions. The effect of temperature, with and without transport limitations, on pyrolysis product distribution and on bio-oil composition, was studied. In thin-film pyrolysis, non-condensable gases and bio-oil yields increased with temperature, while char yield decreased. Within the thin-film derived bio-oil, anhydrosugars (*viz*. LGA and LGO) remained dominant at 300 ºC, while around 400 ºC, furans (*viz*. 5-HMF and furfural) occupied a major percentage of bio-oil. At the higher pyrolysis temperature (~ 500 ºC), bio-oil became rich in light oxygenates (viz. FA and MG). Thus, the decomposition of glucose under reaction-controlled pyrolysis condition was initiated by dehydration reactions, followed by ring-opening/closing reactions (~ 400 ºC) and at around 500 ºC, fragmentation reactions became more facile.

Powder form of glucose produced similar yield of non-condensable gases but higher yield of bio-oil and lower yield of char as compared to that of glucose thin-film, at all temperatures. Amongst the bio-oil compounds, LGA decreased slightly with pyrolysis temperatures but increased significantly with increasing size of glucose particles. LGO decreased monotonically with temperature and particle size. Major furans (*viz.* HMF and furfural) and light oxygenates (viz. FA and MG) increased monotonically with increase in temperature and particle size. Further, the yield of char in glucose powders was significantly lower than that in glucose thin-film, possibly because of the repolymerization of anhydrosugars/pyrans species in glucose thin-film due to uniform temperature within the film. In summary the current study systematically showed that by tuning temperature and particle size, the selectivity of individual compounds in bio-oil can be altered. Such analysis would also help in optimizing operating conditions for obtaining desired yield and composition of bio-oil for different feedstocks in the pyrolysis process. Moreover, the current experimental data of glucose pyrolysis without and with transport-limitations would be utilized to validate the in house developed particle scale model, which takes into account pyrolysis reaction chemistry (as reaction kinetics) and transport to enable us understand the reaction-transport interplay during the pyrolysis process.

Acknowledgement

This research is supported by the Ministry of Education, Singapore, under the Academic Research Fund (AcRF) Tier-2 grant (Grant No. T2-1-082).

Conflicts of Interest

There are no conflicts of interest to declare.

Supporting Information

The supporting information is provided for the experimental setup of glucose thin-film/powder pyrolysis (Figure S1). The effect of temperatures on individual bio-oil compounds under

reaction-controlled pyrolysis conditions and a reaction map of glucose decomposition at different temperatures are shown (Figures S2 to S4). Further, the summary of identified products in glucose thin-film and powder pyrolysis experiments and comparison of anhydrosugars/pyran yields versus char yields in glucose thin-film/powder pyrolysis experiments are presented in Tables T1 and T2, respectively.

References

1. Collard, F.-X.; Blin, J., A review on pyrolysis of biomass constituents: Mechanisms and composition of the products obtained from the conversion of cellulose, hemicelluloses and lignin. *Renew. Sus. Energ. Rev.* **2014,** 38, 594-608.
2. Anex, R. P.; Aden, A.; Kazi, F. K.; Fortman, J.; Swanson, R. M.; Wright, M. M.; Satrio, J. A.; Brown, R. C.; Daugaard, D. E.; Platon, A.; Kothandaraman, G.; Hsu, D. D.; Dutta, A., Techno-economic comparison of biomass-to-transportation fuels via pyrolysis, gasification, and biochemical pathways. *Fuel* **2010,** 89, Supplement 1, S29-S35.
3. Bridgwater, A. V., Review of fast pyrolysis of biomass and product upgrading. *Biomass Bioenergy* **2012,** 38, 68-94.
4. Huber, G. W.; Iborra, S.; Corma, A., Synthesis of Transportation Fuels from Biomass: Chemistry, Catalysts, and Engineering. *Chem. Rev.* **2006,** 106, (9), 4044-4098.
5. Westerhof, R. J. M.; Oudenhoven, S. R. G.; Marathe, P. S.; Engelen, M.; Garcia-Perez, M.; Wang, Z.; Kersten, S. R. A., The interplay between chemistry and heat/mass transfer during the fast pyrolysis of cellulose. *React. Chem. Eng.* **2016,** 1, (5), 555-566.
6. Serrano-Ruiz, J. C.; Dumesic, J. A., Catalytic routes for the conversion of biomass into liquid hydrocarbon transportation fuels. *Energy Environ. Sci.* **2011,** 4, (1), 83-99.

7. Bridgwater, A. V.; Toft, A. J.; Brammer, J. G., A techno-economic comparison of power production by biomass fast pyrolysis with gasification and combustion. *Renew. Sus. Energ. Rev.* **2002,** 6, (3), 181-246.
8. Tsai, W. T.; Lee, M. K.; Chang, Y. M., Fast pyrolysis of rice husk: Product yields and compositions. *Bioresource Technol.* **2007,** 98, (1), 22-28.
9. Acıkgoz, C.; Onay, O.; Kockar, O. M., Fast pyrolysis of linseed: product yields and compositions. *J. Anal. Appl. Pyrolysis* **2004,** 71, (2), 417-429.
10. Greenhalf, C. E.; Nowakowski, D. J.; Harms, A. B.; Titiloye, J. O.; Bridgwater, A. V., A comparative study of straw, perennial grasses and hardwoods in terms of fast pyrolysis products. *Fuel* **2013,** 108, 216-230.
11. Garcia-Perez, M.; Wang, X. S.; Shen, J.; Rhodes, M. J.; Tian, F.; Lee, W.-J.; Wu, H.; Li, C.-Z., Fast Pyrolysis of Oil Mallee Woody Biomass: Effect of Temperature on the Yield and Quality of Pyrolysis Products. *Ind. Eng. Chem. Res.* **2008,** 47, (6), 1846-1854.
12. Uzun, B. B.; Pütün, A. E.; Pütün, E., Fast pyrolysis of soybean cake: Product yields and compositions. *Bioresource Technol.* **2006,** 97, (4), 569-576.
13. Ozbay, N.; Pütün, A. E.; Pütün, E., Bio-oil production from rapid pyrolysis of cottonseed cake: product yields and compositions. *Int. J. Energy Res.* **2006,** 30, (7), 501-510.
14. Özbay, G.; Pekgözlü, A. K.; Ozcifci, A., The effect of heat treatment on bio-oil properties obtained from pyrolysis of wood sawdust. *Eur. J. Wood Wood Prod.* **2015,** 73, (4), 507-514.
15. Mortensen, P. M.; Grunwaldt, J. D.; Jensen, P. A.; Knudsen, K. G.; Jensen, A. D., A review of catalytic upgrading of bio-oil to engine fuels. *Appl. Catal., A* **2011,** 407, (1), 1-19.
16. Moraes, M. S. A.; Georges, F.; Almeida, S. R.; Damasceno, F. C.; Maciel, G. P. d. S.; Zini, C. A.; Jacques, R. A.; Caramão, E. B., Analysis of products from pyrolysis of Brazilian sugar cane straw. *Fuel Process. Technol.* **2012,** 101, 35-43.

17. Czernik, S.; Bridgwater, A. V., Overview of Applications of Biomass Fast Pyrolysis Oil. *Energy Fuels* **2004,** 18, (2), 590-598.
18. Mukherjee, A.; Debnath, B.; Ghosh, S. K., A Review on Technologies of Removal of Dioxins and Furans from Incinerator Flue Gas. *Procedia Environ. Sci.* **2016,** 35, (Supplement C), 528-540.
19. Paulsen, A. D.; Mettler, M. S.; Dauenhauer, P. J., The Role of Sample Dimension and Temperature in Cellulose Pyrolysis. *Energy Fuels* **2013,** 27, (4), 2126-2134.
20. Mettler, M. S.; Mushrif, S. H.; Paulsen, A. D.; Javadekar, A. D.; Vlachos, D. G.; Dauenhauer, P. J., Revealing pyrolysis chemistry for biofuels production: Conversion of cellulose to furans and small oxygenates. *Energy Environ. Sci.* **2012,** 5, (1), 5414-5424.
21. Mettler, M. S.; Paulsen, A. D.; Vlachos, D. G.; Dauenhauer, P. J., Pyrolytic conversion of cellulose to fuels: levoglucosan deoxygenation via elimination and cyclization within molten biomass. *Energy Environ. Sci.* **2012,** 5, (7), 7864-7868.
22. Park, W. C.; Atreya, A.; Baum, H. R., Experimental and theoretical investigation of heat and mass transfer processes during wood pyrolysis. *Combust. Flame* **2010,** 157, (3), 481-494.
23. Ciesielski, P. N.; Crowley, M. F.; Nimlos, M. R.; Sanders, A. W.; Wiggins, G. M.; Robichaud, D.; Donohoe, B. S.; Foust, T. D., Biomass Particle Models with Realistic Morphology and Resolved Microstructure for Simulations of Intraparticle Transport Phenomena. *Energy Fuels* **2015,** 29, (1), 242-254.
24. Babu, B. V.; Chaurasia, A. S., Heat transfer and kinetics in the pyrolysis of shrinking biomass particle. *Chem. Eng. Sci.* **2004,** 59, (10), 1999-2012.
25. Anca-Couce, A.; Zobel, N., Numerical analysis of a biomass pyrolysis particle model: Solution method optimized for the coupling to reactor models. *Fuel* **2012,** 97, 80-88.

26. Haseli, Y.; van Oijen, J. A.; de Goey, L. P. H., Predicting the pyrolysis of single biomass particles based on a time and space integral method. *J. Anal. Appl. Pyrolysis* **2012,** 96, 126-138.
27. Haseli, Y.; van Oijen, J. A.; de Goey, L. P. H., Numerical study of the conversion time of single pyrolyzing biomass particles at high heating conditions. *Chem. Eng. J.* **2011,** 169, (1–3), 299-312.
28. Haseli, Y.; van Oijen, J. A.; de Goey, L. P. H., Modeling biomass particle pyrolysis with temperature-dependent heat of reactions. *J. Anal. Appl. Pyrolysis* **2011,** 90, (2), 140-154.
29. Krumm, C.; Pfaendtner, J.; Dauenhauer, P. J., Millisecond Pulsed Films Unify the Mechanisms of Cellulose Fragmentation. *Chem. Mater.* **2016,** 28, (9), 3108-3114.
30. Zhu, C.; Krumm, C.; Facas, G. G.; Neurock, M.; Dauenhauer, P. J., Energetics of cellulose and cyclodextrin glycosidic bond cleavage. *React. Chem. Eng.* **2017,** 2, (2), 201-214.
31. Lin, Y.-C.; Cho, J.; Tompsett, G. A.; Westmoreland, P. R.; Huber, G. W., Kinetics and Mechanism of Cellulose Pyrolysis. *J. Phys. Chem. C* **2009,** 113, (46), 20097-20107.
32. Zhang, X.; Li, J.; Yang, W.; Blasiak, W., Formation Mechanism of Levoglucosan and Formaldehyde during Cellulose Pyrolysis. *Energy Fuels* **2011,** 25, (8), 3739-3746.
33. Zhang, X.; Yang, W.; Dong, C., Levoglucosan formation mechanisms during cellulose pyrolysis. *J. Anal. Appl. Pyrolysis* **2013,** 104, (Supplement C), 19-27.
34. Assary, R. S.; Curtiss, L. A., Thermochemistry and Reaction Barriers for the Formation of Levoglucosenone from Cellobiose. *ChemCatChem* **2012,** 4, (2), 200-205.
35. Assary, R. S.; Curtiss, L. A., Comparison of Sugar Molecule Decomposition through Glucose and Fructose: A High-Level Quantum Chemical Study. *Energy Fuels* **2012,** 26, (2), 1344-1352.

36. Seshadri, V.; Westmoreland, P. R., Concerted Reactions and Mechanism of Glucose Pyrolysis and Implications for Cellulose Kinetics. *J. Phys. Chem. A* **2012,** 116, (49), 11997-12013.

37. Huang, J.; Liu, C.; Wei, S.; Huang, X.; Li, H., Density functional theory studies on pyrolysis mechanism of β-d-glucopyranose. *J. Mol. Struct.: THEOCHEM* **2010,** 958, (1), 64-70.

38. Zhang, M.; Geng, Z.; Yu, Y., Density Functional Theory (DFT) Study on the Dehydration of Cellulose. *Energy Fuels* **2011,** 25, (6), 2664-2670.

39. Nimlos, M. R.; Blanksby, S. J.; Qian, X.; Himmel, M. E.; Johnson, D. K., Mechanisms of Glycerol Dehydration. *J. Phys. Chem. A* **2006,** 110, (18), 6145-6156.

40. Mayes, H. B.; Broadbelt, L. J., Unraveling the Reactions that Unravel Cellulose. *J. Phys. Chem. A* **2012,** 116, (26), 7098-7106.

41. Maduskar, S.; Facas, G. G.; Papageorgiou, C.; Williams, C. L.; Dauenhauer, P. J., Five Rules for Measuring Biomass Pyrolysis Rates: Pulse-Heated Analysis of Solid Reaction Kinetics of Lignocellulosic Biomass. *ACS Sustain. Chem. Eng.* **2018,** 6, (1), 1387-1399.

42. Zhou, X.; Nolte, M. W.; Mayes, H. B.; Shanks, B. H.; Broadbelt, L. J., Experimental and Mechanistic Modeling of Fast Pyrolysis of Neat Glucose-Based Carbohydrates. 1. Experiments and Development of a Detailed Mechanistic Model. *Ind. Eng. Chem. Res.* **2014,** 53, (34), 13274-13289.

43. Mayes, H. B.; Nolte, M. W.; Beckham, G. T.; Shanks, B. H.; Broadbelt, L. J., The Alpha–Bet(a) of Glucose Pyrolysis: Computational and Experimental Investigations of 5-Hydroxymethylfurfural and Levoglucosan Formation Reveal Implications for Cellulose Pyrolysis. *Acs Sustain. Chem. Eng.* **2014,** 2, (6), 1461-1473.

44. Zhu, C.; Maduskar, S.; Paulsen, A. D.; Dauenhauer, P. J., Alkaline-Earth-Metal-Catalyzed Thin-Film Pyrolysis of Cellulose. *ChemCatChem* **2016,** 8, (4), 818-829.

45. Ponder, G. R.; Richards, G. N., Pyrolysis of some 13C-labeled glucans: a mechanistic study. *Carbohydr. Res.* **1993,** 244, (1), 27-47.
46. Patwardhan, P. R.; Satrio, J. A.; Brown, R. C.; Shanks, B. H., Product distribution from fast pyrolysis of glucose-based carbohydrates. *J. Anal. Appl. Pyrolysis* **2009,** 86, (2), 323-330.
47. Paine Iii, J. B.; Pithawalla, Y. B.; Naworal, J. D., Carbohydrate pyrolysis mechanisms from isotopic labeling: Part 4. The pyrolysis of d-glucose: The formation of furans. *J. Anal. Appl. Pyrolysis* **2008,** 83, (1), 37-63.
48. Ponder, G. R.; Richards, G. N., Pyrolysis of inulin, glucose and fructose. *Carbohydr. Res.* **1993,** 244, (2), 341-359.
49. Perez Locas, C.; Yaylayan, V. A., Isotope Labeling Studies on the Formation of 5-(Hydroxymethyl)-2-furaldehyde (HMF) from Sucrose by Pyrolysis-GC/MS. *J. Agric. Food Chem.* **2008,** 56, (15), 6717-6723.
50. Karinen, R.; Vilonen, K.; Niemelä, M., Biorefining: Heterogeneously Catalyzed Reactions of Carbohydrates for the Production of Furfural and Hydroxymethylfurfural. *ChemSusChem* **2011,** 4, (8), 1002-1016.
51. Assary, R. S.; Redfern, P. C.; Greeley, J.; Curtiss, L. A., Mechanistic Insights into the Decomposition of Fructose to Hydroxy Methyl Furfural in Neutral and Acidic Environments Using High-Level Quantum Chemical Methods. *J. Phys. Chem. B* **2011,** 115, (15), 4341-4349.
52. Lin, X.; Qu, Y.; Lv, Y.; Xi, Y.; Phillips, D. L.; Liu, C., The first dehydration and the competing reaction pathways of glucose homogeneously and heterogeneously catalyzed by acids. *Phys. Chem. Chem. Phys.* **2013,** 15, (8), 2967-2982.

53. Hu, B.; Lu, Q.; Jiang, X.-y.; Dong, X.-c.; Cui, M.-s.; Dong, C.-q.; Yang, Y.-p., Insight into the Formation of Anhydrosugars in Glucose Pyrolysis: A Joint Computational and Experimental Investigation. *Energy Fuels* **2017,** 31, (8), 8291-8299.
54. Sharma, A.; Pareek, V.; Wang, S.; Zhang, Z.; Yang, H.; Zhang, D., A phenomenological model of the mechanisms of lignocellulosic biomass pyrolysis processes. *Comput. Chem. Eng.* **2014,** 60, 231-241.
55. Hutchinson, C. P.; Lee, Y. J., Evaluation of Primary Reaction Pathways in Thin-Film Pyrolysis of Glucose Using 13C Labeling and Real-Time Monitoring. *ACS Sustain. Chem. Eng*. **2017**, 5 (10) 8796-8803.

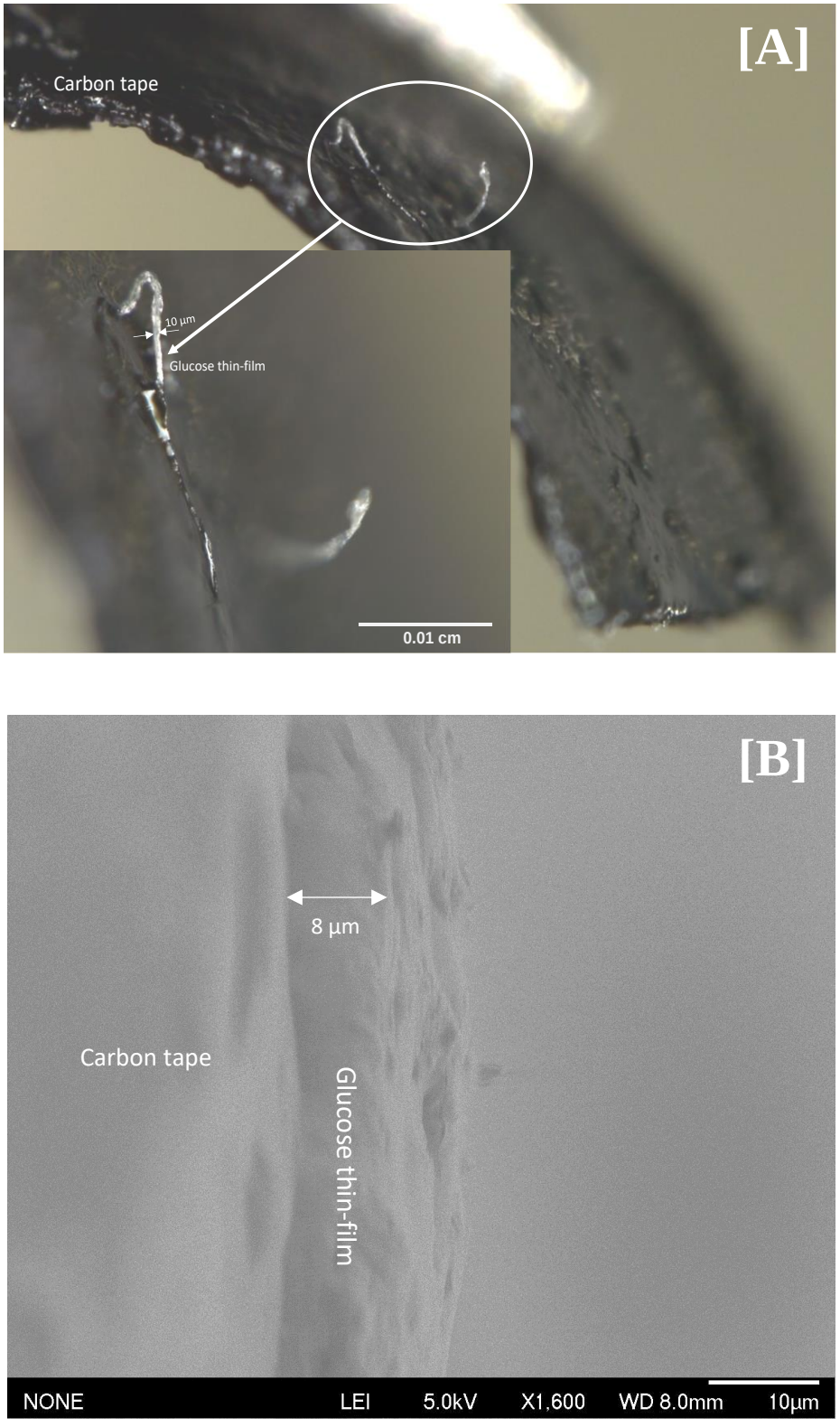

Figure 1: Glucose thin-film images acquired from [A] Digital Microscope [B] Scanning Electron Microscope (*cross-sectional SEM image*)

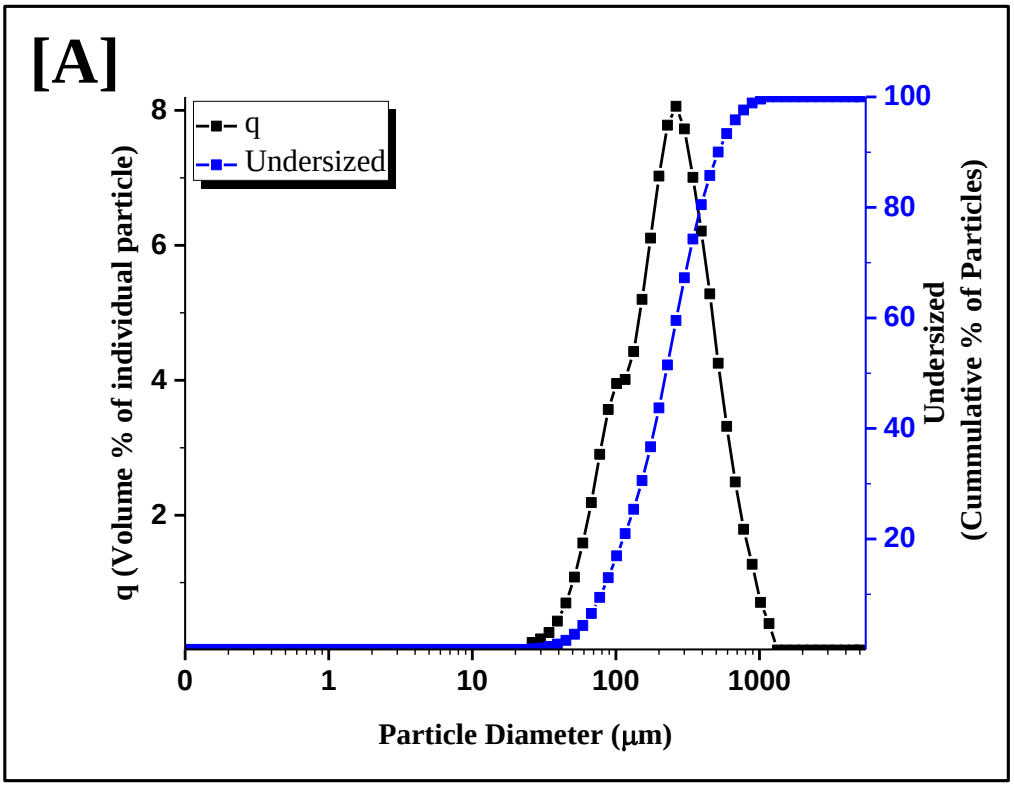

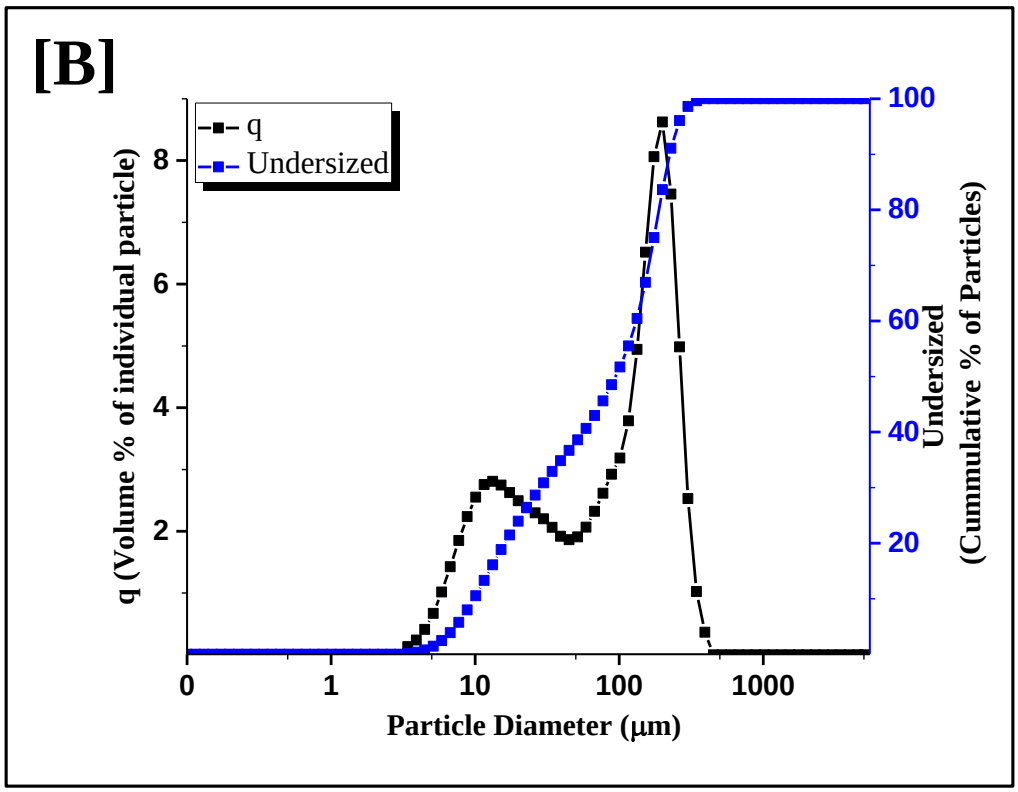

Figure 2: Particle size distribution of glucose powders measured by Partica LA-960 series

[A] Particle size: 83 – 523 μm [B] Particle size: 10 – 262 μm

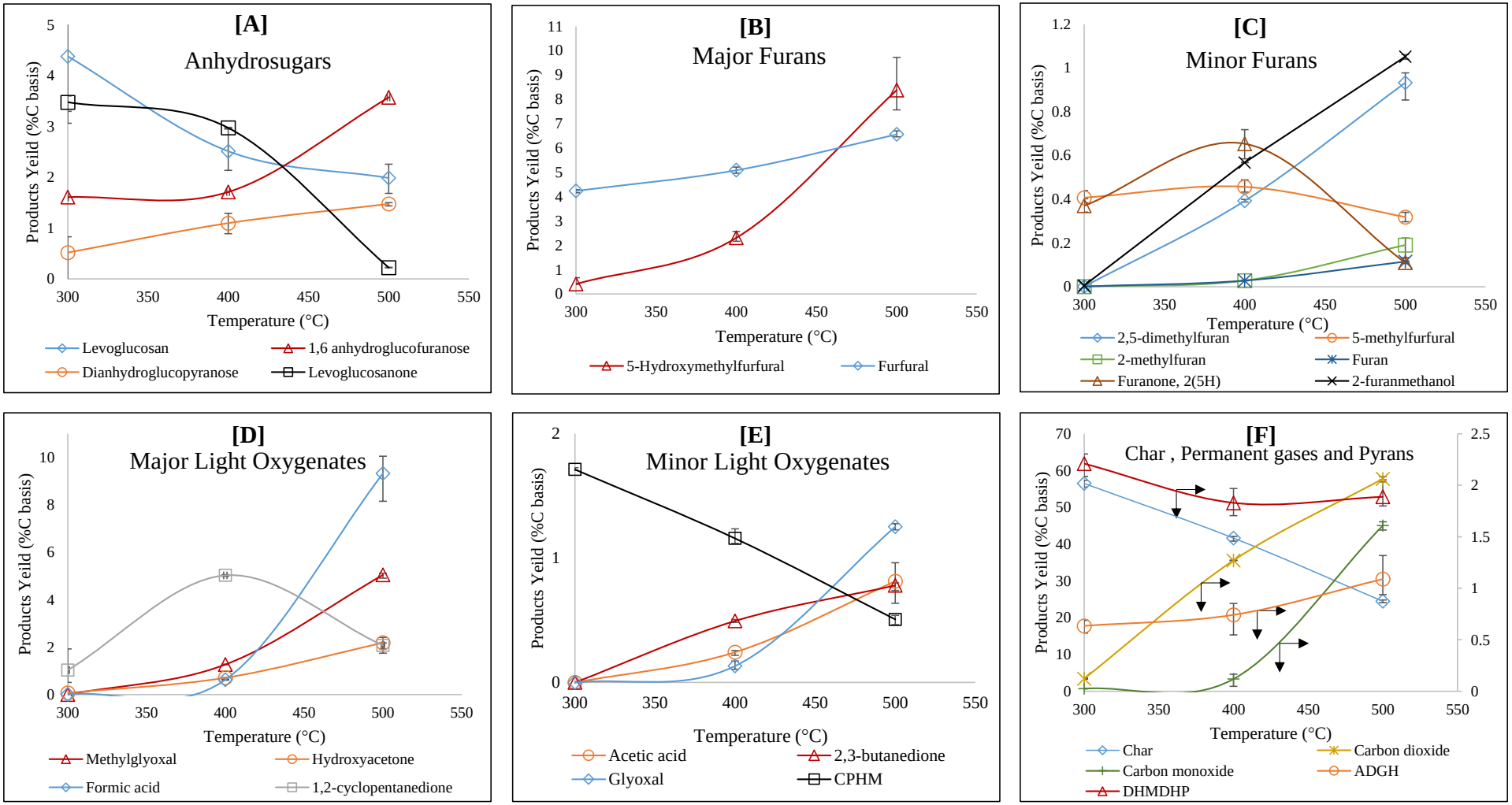

Figure 3: Glucose thin-film pyrolysis: Effect of pyrolysis temperatures on product yield. Nomenclature is shown for pyrolysis products CPHM: 2-hydroxy-3-methyl-2-cyclopenten-1-one; ADGH: 1, 5-anhydro-4-deoxy-D-glycerohex-1-en-3-ulose; DHMDHP: 2,3-dihydro-3,5-dihydroxy-6-methyl-4HPyran- 4-on

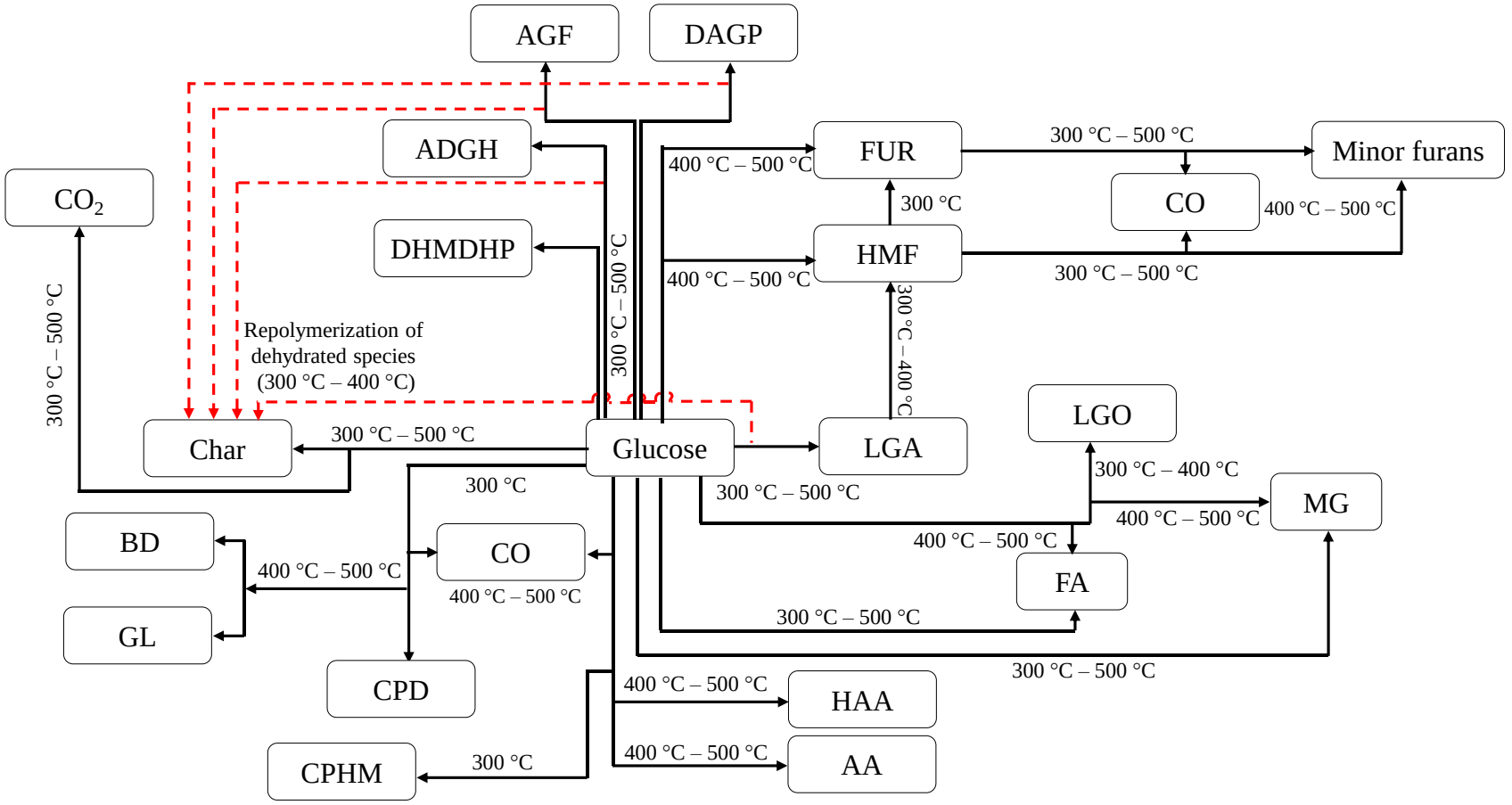

Figure 4: Reaction map of glucose-derived products during thin-film pyrolysis. Nomenclature shown in the figure for products. LGA: Levoglucosan; LGO: Levoglucosenone; AGF: 1, 6-anhydroglucofuranose; DAGP: Dianhydroglucopyranose; ADGH: 1,5-anhydro-4-deoxy-D-glycero-hex-1-en-3-ulose; DHMDHP: 2,3-dihydro-3,5-dihydroxy-6-methyl-4H-Pyran-4-one; HMF: 5-Hydroxymethylfurfural; FUR: Furfural; FA: Formic acid; MG: Methyl glyoxal; HAA: Hydroxyacetone; AA: Acetic acid; CPD: Cyclopentanedione; CPHM: 2-hydroxy-3-methyl-2-cyclopenten-1-one; BD: Butanedione; GL: Glyoxal; CO: Carbon monoxide; CO_2: Carbon dioxide

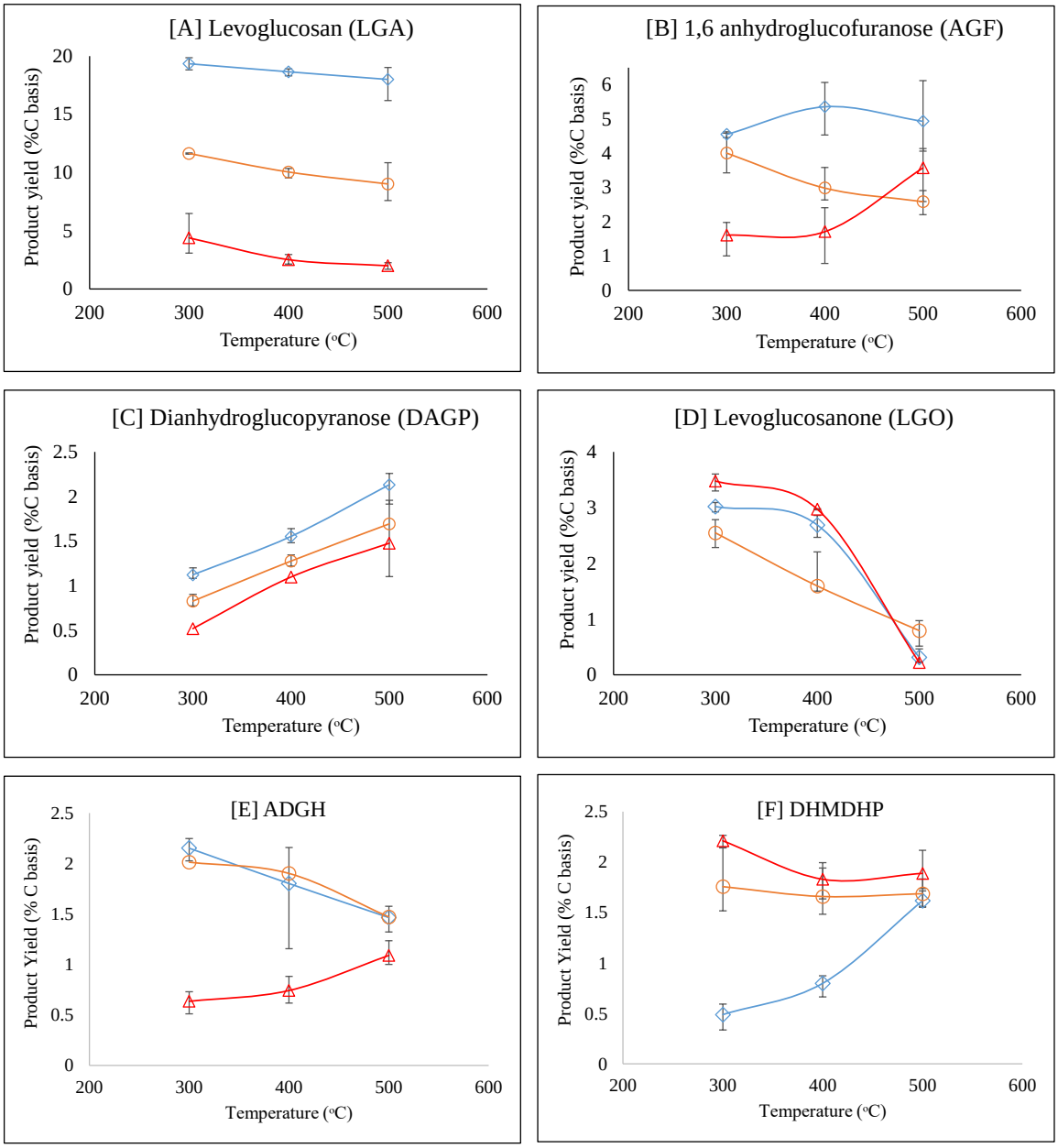

Figure 5: Effect of glucose particle size and pyrolysis temperatures on anhydrosugar and pyran yields. Nomenclature shown in figure for product, ADGH: 1,5-anhydro-4-deoxy-D-glycero-hex-1-en-3-ulose; DHMDHP: 2,3-dihydro-3,5-dihydroxy-6-methyl-4H-Pyran-4-one.

(For products yields red colour depicts glucose thin-film of 8 – 10 µm, yellow and blue colours for glucose powders of 10 – 262 µm and 83 – 523 µm, respectively)

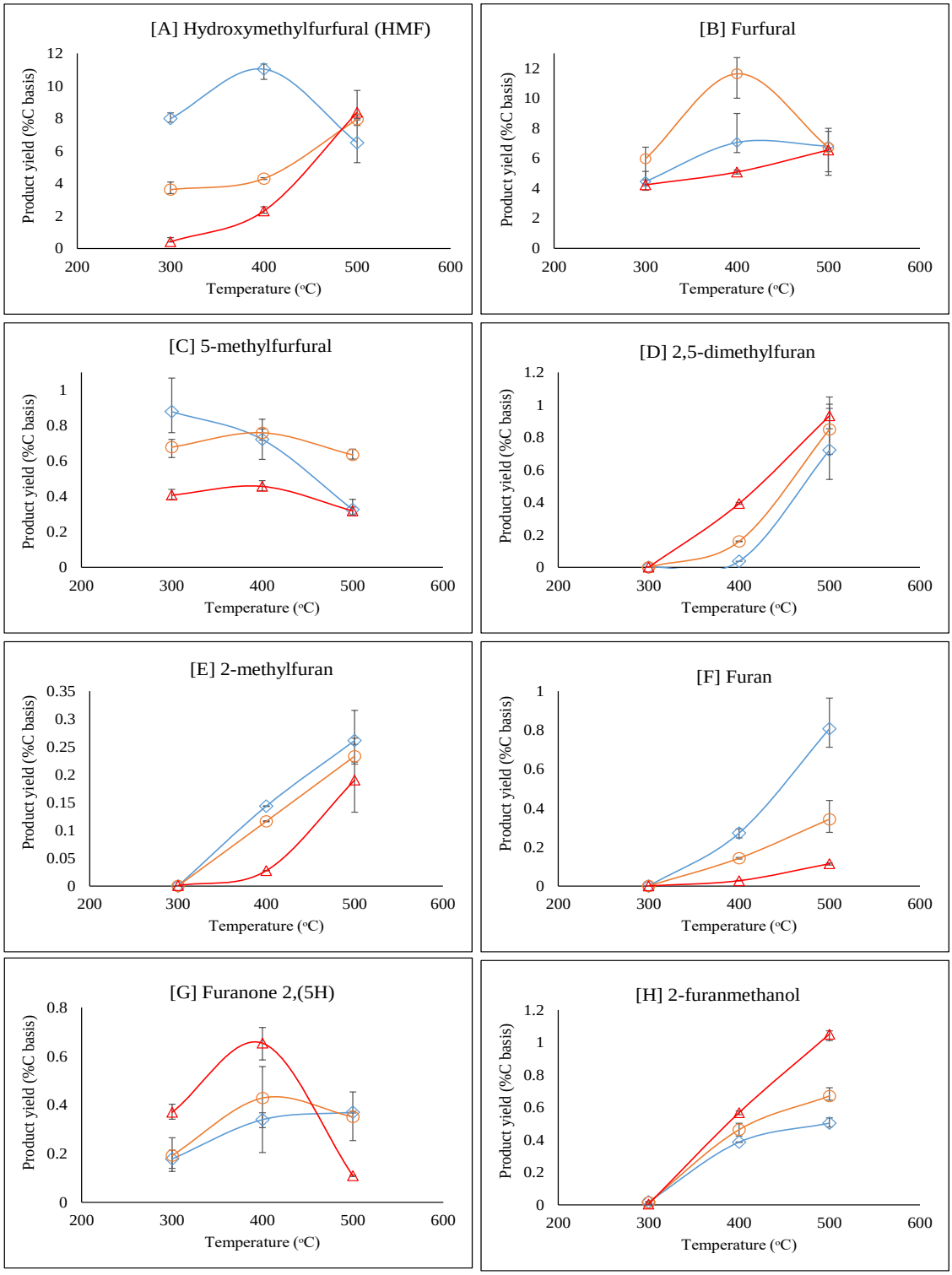

Figure 6: Effect of glucose particle size and pyrolysis temperatures on furanic compound yields (For products yields red colour depicts glucose thin-film of 8 – 10 µm, yellow and blue colours for glucose powders of 10 – 262 µm and 83 – 523 µm, respectively)

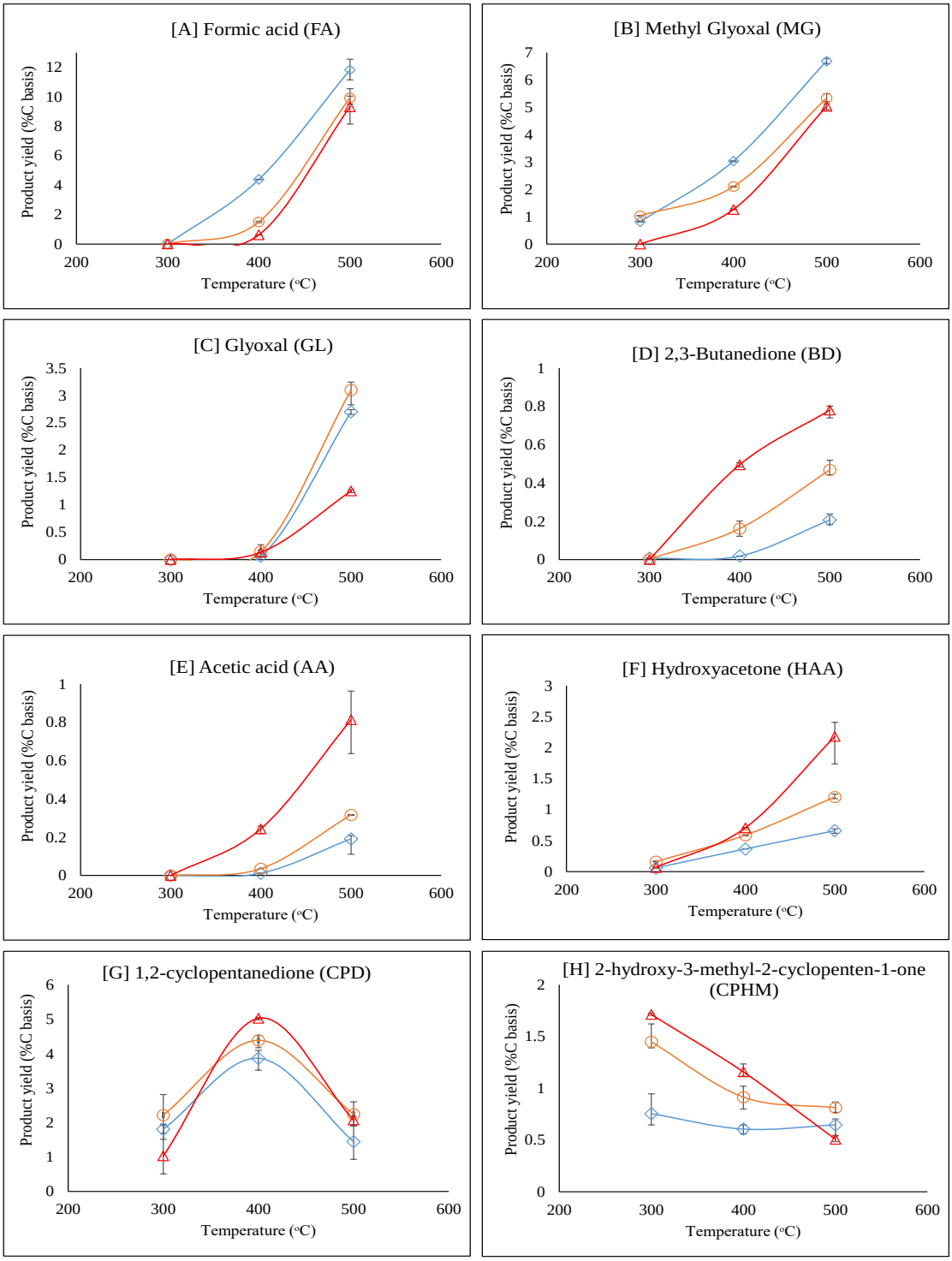

Figure 7: Effect of glucose particle size and pyrolysis temperatures on light oxygenates yields. (For products yields red colour depicts glucose thin-film of 8 – 10 µm, yellow and blue colours for glucose powders of 10 – 262 µm and 83 – 523 µm, respectively)

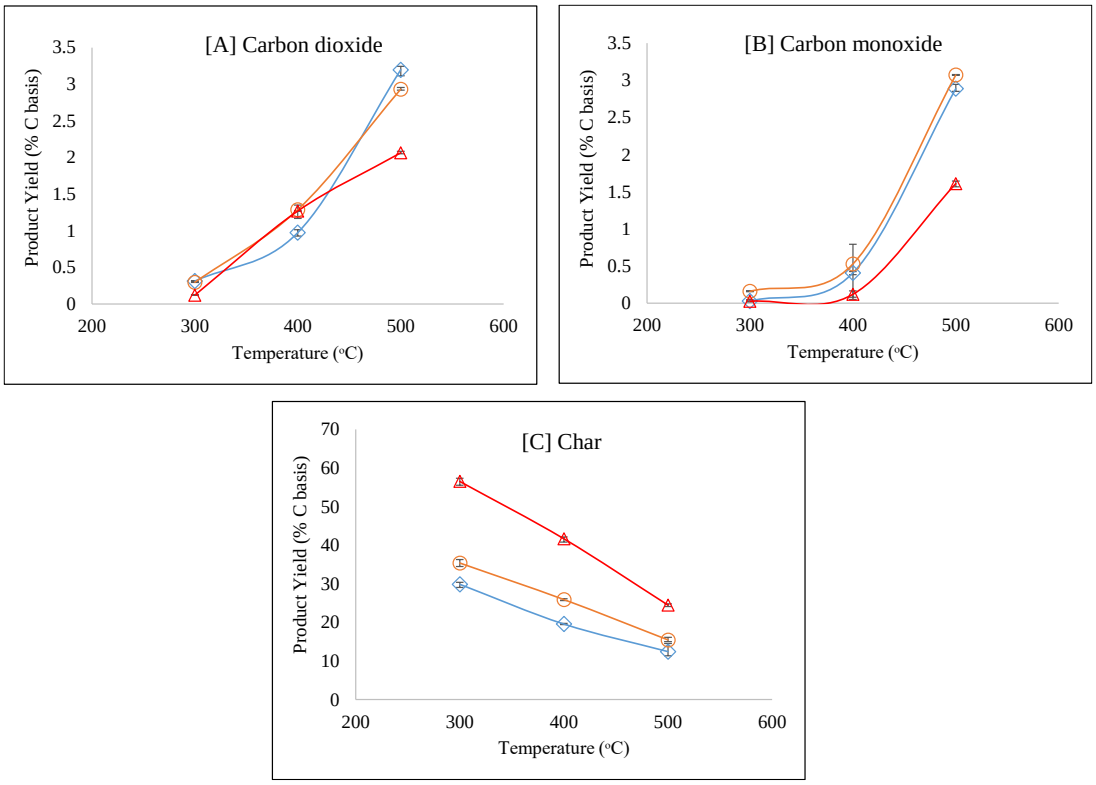

Figure 8: Effect of glucose particle size and pyrolysis temperatures on non-condensable gases and char yields

(For products yields red colour depicts glucose thin-film of 8 – 10 µm, yellow and blue colours for glucose powders of 10 – 262 µm and 83 – 523 µm, respectively)

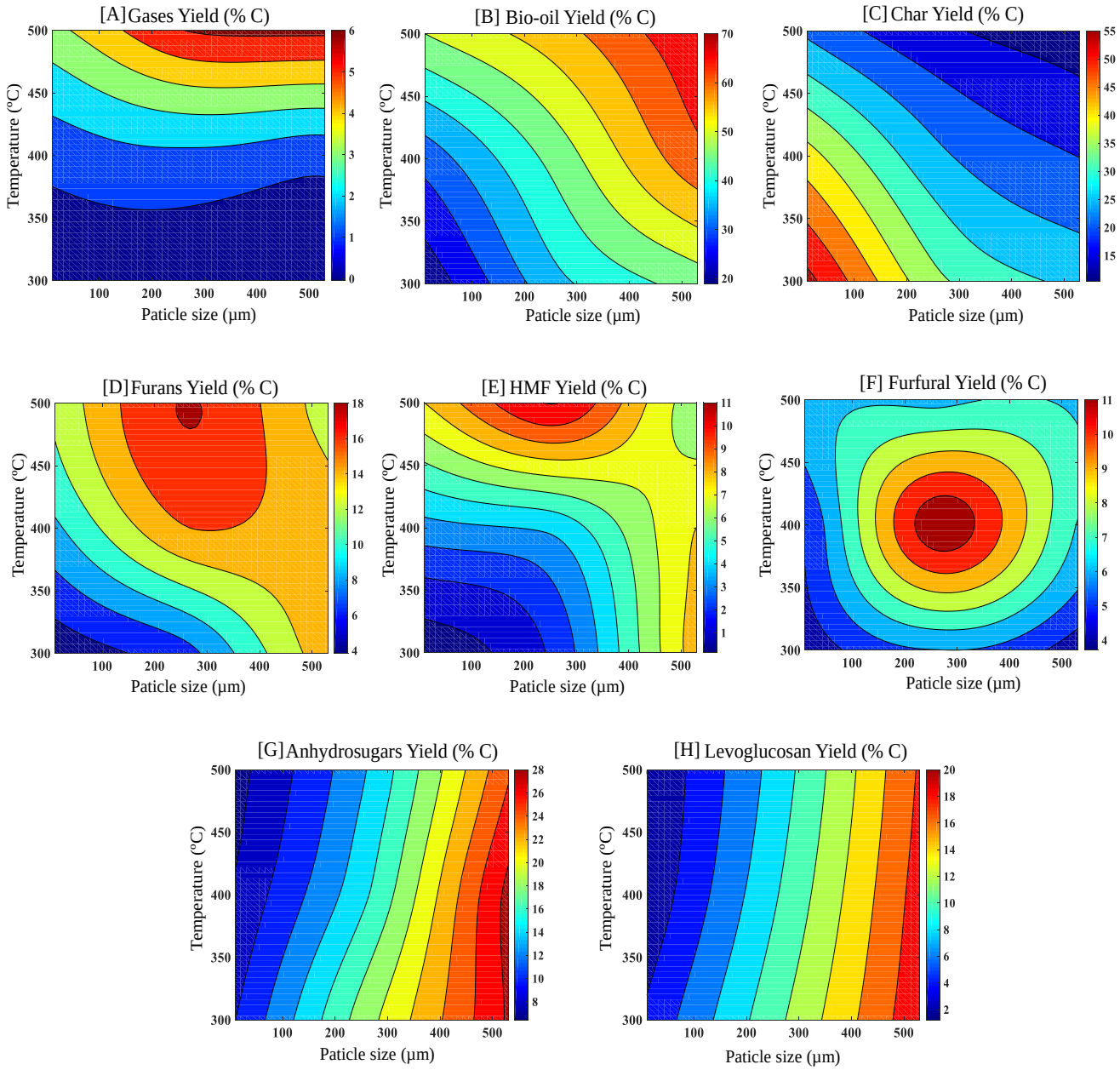

Figure 9: Yields of [A] Non-condensable gases [B] Bio-oil [C] Char [D] Furans [E] 5-HMF [F] Furfural [G] Anhydrosugars and [H] Levoglucosan versus pyrolysis temperature and glucose particle size

Table 1 [A]: Glucose thin-film and powder pyrolysis: Product distribution

Temperature (°C)	*Glucose thin-film (8 – 10 µm): Product yield (% C basis)*		
	Non-condensable gases	Bio-oil	Char
300	0.15 ± 0.01	21.5 ± 1.71	56.5 ± 0.91
400	1.38 ± 0.11	31.8 ± 0.81	41.6 ± 0.65
500	3.7 ± 0.02	50.2 ± 0.95	24.5 ± 0.35
Temperature (°C)	*Glucose powder (10 – 262 µm): Product yield (% C basis)*		
	Non-condensable gases	Bio-oil	Char
300	0.45 ± 0.01	38.2 ± 0.32	35.3 ± 0.89
400	1.81 ± 0.22	47.3 ± 0.22	25.9 ± 0.22
500	5.8 ± 0.01	58.4 ± 0.31	15.4 ± 0.57
Temperature (°C)	*Glucose powder (83 – 523 µm): Product yield (% C basis)*		
	Non-condensable gases	Bio-oil	Char
300	0.33 ± 0.01	47.8 ± 0.14	29.8 ± 0.68
400	1.98 ± 0.03	63.7 ± 0.17	19.5 ± 0.14
500	6.1 ± 0.05	64.7 ± 0.34	12.4 ± 1.59

Table 1 [B]: Glucose thin-film and powder pyrolysis: Bio-oil composition

Temperature (°C)	*Glucose thin-film (8 – 10 µm): Bio-oil composition (% C basis)*			
	Anhydrosugars	Pyrans	Furans	Light oxygenates
300	46.8 ± 0.68	14.5 ± 0.08	25.4 ± 0.05	13.2 ± 0.15
400	26.0 ± 0.51	13.8 ± 0.14	29.8 ± 0.11	30.3 ± 0.02
500	14.4 ± 0.9	6.67 ± 0.15	35.1 ± 0.20	43.7 ± 0.29
Temperature (°C)	*Glucose Powder (10 – 262 µm): Bio-oil composition (% C basis)*			
	Anhydrosugars	Pyrans	Furans	Light oxygenates
300	49.7 ± 0.35	10.0 ± 0.37	27.4 ± 0.22	12.7 ± 0.70
400	33.6 ± 0.25	7.52 ± 0.18	38.1 ± 0.20	20.8 ± 0.57
500	24.1 ± 0.65	5.40 ± 0.42	30.4 ± 1.97	40.1 ± 1.35
Temperature (°C)	*Glucose Powder (83 – 523 µm): Bio-oil composition (% C basis)*			
	Anhydrosugars	Pyrans	Furans	Light oxygenates
300	58.6 ± 0.19	5.84 ± 0.12	28.3 ± 0.23	7.2 ± 0.07
400	44.3 ± 0.33	4.85 ± 0.30	31.3 ± 0.21	19.4 ± 0.04
500	36.4 ± 0.68	5.25 ± 0.10	23.4 ± 0.40	34.9 ± 0.18